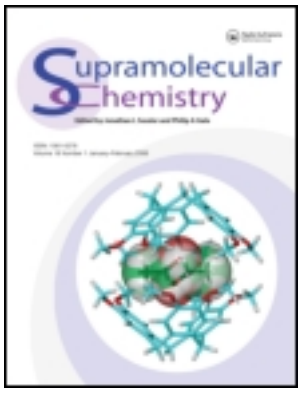

Supramolecular Chemistry
Publication details, including instructions for authors and subscription information:
http://www.tandfonline.com/loi/gsch20

Solvatochromism of triarylbilindiones: far-red-absorbing bilindiones formed in aprotic amides and amines

Nao Furuta [a] & Tadashi Mizutani [a]

[a] Department of Molecular Chemistry and Biochemistry, Faculty of Science and Engineering, Doshisha University, Tatara-miyakotani, Kyotanabe, Kyoto, 610-0321, Japan

Available online: 27 Aug 2010

To cite this article: Nao Furuta & Tadashi Mizutani (2011): Solvatochromism of triarylbilindiones: far-red-absorbing bilindiones formed in aprotic amides and amines, Supramolecular Chemistry, 23:01-02, 74-82

To link to this article: http://dx.doi.org/10.1080/10610278.2010.510559

Supramolecular Chemistry
Vol. 23, Nos. 1–2, January–February 2011, 74–82

Taylor & Francis
Taylor & Francis Group

Solvatochromism of triarylbilindiones: far-red-absorbing bilindiones formed in aprotic amides and amines

Nao Furuta and Tadashi Mizutani*

Department of Molecular Chemistry and Biochemistry, Faculty of Science and Engineering, Doshisha University, Tatara-miyakotani, Kyotanabe, Kyoto 610-0321, Japan

(*Received 2 June 2010; final version received 20 July 2010*)

Solvatochromism of triarylbilindiones was investigated to shed light on the mechanism and interactions involved in the phytochrome P_r–P_{fr} isomerisation. 1,19,21,24-Tetrahydro-5,10,15-tri(4-cyanophenyl)bilin-1,19-dione exhibited an electronic absorption maximum at 631 nm in toluene, while it exhibited the absorption maximum at 729 nm in *N*,*N*-dimethylformamide. A similar far-red-absorbing bilindione (P_{fr}) was formed in aprotic amides such as *N*,*N*-dimethylacetamide and 1-methylpyrrolidone, but was not formed in protic amides such as formamide and *N*-methylformamide. The P_{fr} was formed in the presence of a relatively high concentration (~0.1 M) of amines such as butylamine, 1,2-ethanediamine and piperidine in methanol. The formation of P_{fr} in amides was inhibited by the addition of protic polar solvents, in particular hydrogen donor solvents such as 2,2,2-trifluoroethanol and methanol, while the formation of P_{fr} in the presence of amines was favourable in polar solvents. Tricyanophenyl bilindione tends to form P_{fr} than does tri(4-methoxyphenyl)bilindione. These observations suggest that the bilindiones act as hydrogen donors to form a hydrogen bond complex with amides or amines.

Keywords: bilindione; solvatochromism; amide; hydrogen bond

1. Introduction

Hydrogen bonding of a dye with surrounding molecules causes structural changes in the dye molecule, and also changes in optical properties of the dye. One of the sophisticated examples is the photoreceptor, phytochrome, where the light induces isomerisation of the linear tetrapyrrole (*1*) and concomitantly induces the structural changes (hydrogen-bonding formation/cleavage) in the apoprotein.

Phytochrome in its resting form absorbs red light ($\lambda_{max} = 660$ nm), P_r, while that in the biologically activated form absorbs far-red light ($\lambda_{max} = 730$ nm), P_{fr}. The structures of phytochromes have been elucidated by use of X-ray crystallography, UV–vis spectroscopy, NMR spectroscopy and resonance Raman spectroscopy (*2*). These studies revealed that the P_r form has 4*Z*, 9*Z*, 15*Z* double bond configurations while the P_{fr} form has 4*Z*, 9*Z*, 15*E* configurations. However, detailed interactions of the dye with the apoprotein have not been fully elucidated, due to the small quantities of phytochrome obtained from plants and the transient nature of the P_{fr} species.

We report here that 5,10,15-triarylbilindiones showed solvatochromism similar to the spectral changes observed for phytochrome, where the bilindiones absorb red light ($\lambda_{max} = 630$ nm) in protic polar solvents and apolar solvents, while it absorbs far-red light ($\lambda_{max} = 730$ nm) in aprotic polar solvents such as DMF, 1-methylpyrrolidone and DMSO. The spectral shifts were attributed to the hydrogen bond between the NH group of the D-ring pyrrole and the hydrogen acceptor solvent.

2. Results and discussion

2.1. Synthesis of triarylbilindiones and their structural characterisation

Two triarylbilindiones **1** and **2** (Scheme 1) were prepared from tetraarylporphyrin iron complexes using coupled oxidation reaction (*3*). Details of the synthesis of bilindiones were reported elsewhere (*4*). Compounds **1** and **2** were characterised by ^{1}H NMR and MALDI-TOF mass spectra. The ^{1}H NMR spectra of **1** and **2** in $CDCl_3$ showed four resonances of pyrrole β-protons, indicating that the two dipyrrole units are magnetically equivalent. Thus, the NMR pattern suggests that the bilindiones adopt a symmetric structure. Among the isomers of bilindiones, 4*Z*, 9*Z*, 15*Z*, 5*syn*, 10*syn*, 14*syn*-isomer shown in Scheme 1 is consistent with the NMR spectra. The chemical shifts are similar to those of 5,10,15-triphenylbilindione, whose structure was confirmed to be 4*Z*, 9*Z*, 15*Z*, 5*syn*, 10*syn*, 14*syn*-isomer by X-ray crystallographic studies (*4*). The NH resonances appeared as broad resonances at 8.1 and 12.0 ppm in a 2:1 ratio. The NH resonance appeared at a

*Corresponding author. Email: tmizutan@mail.doshisha.ac.jp

ISSN 1061-0278 print/ISSN 1029-0478 online

DOI: 10.1080/10610278.2010.510559
http://www.informaworld.com

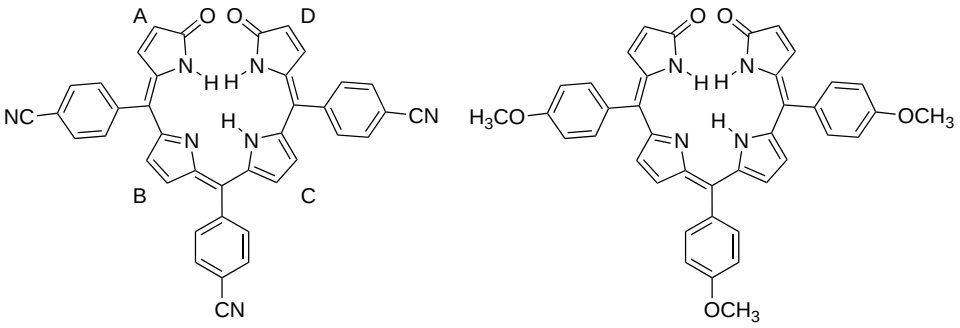

Scheme 1. 5,10,15-Triaryl-1,19,21,24-tetrahydro-1,19-bilindiones **1** and **2**.

lower magnetic field is thus attributed to the B-ring NH, which is hydrogen-bonded to the C-ring N.

2.2 UV–vis spectra of 5,10,15-tri (4-cyanophenyl)bilindione in various solvents including protic and aprotic amides

Figure 1 shows the UV–vis spectra of **1** in toluene, $CHCl_3$, acetone, MeOH, DMSO and DMF. The UV–vis spectrum of **1** in $CHCl_3$ showed two bands in the visible region, a longer wavelength band centred at 631 nm (the Q-band) and a shorter wavelength band centred at 400 nm (the Soret band). The Soret band has a larger absorption coefficient than the Q-band in $CHCl_3$. These features are very similar to the visible spectrum of natural bilindione, aetiobiliverdin-IVγ, for example (*5*). Similar spectra were observed in an apolar solvent (toluene), a polar solvent (acetone) and a protic solvent (MeOH). These red light-absorbing species are called P_r. In DMF, however, the Q-band was shifted to 729 nm, and the absorbance of the Q-band was larger than that of the Soret band. This species absorbs light in the far-red region and is called P_{fr}. In DMSO, two species, P_r and P_{fr}, coexisted.

Formation of the P_{fr} species in DMF was reversible. When a solution of **1** in DMF was diluted with excess $CHCl_3$, and the solution was washed with water several times to remove DMF, the UV–vis spectrum of the resulting $CHCl_3$ solution indicated that the P_r species was regenerated.

Figure 2 shows the UV–vis spectra of **1** in various amides. In protic amides such as formamide and *N*-methylformamide, P_r is predominant, while in aprotic amides such as *N*,*N*-dimethylacetamide, *N*,*N*-dimethylformamide and 1-methylpyrrolidone, P_{fr} is predominant. Figure 3 shows the UV–vis spectra of **1** in mixed solvents, DMF:MeOH (1:1, v/v), DMF:acetone (1:1, v/v), DMF:THF (1:1, v/v), DMF:$CHCl_3$ (1:1, v/v) and DMF:toluene (1:1, v/v). Clearly, inhibition of the formation of P_{fr} occurs in the order MeOH > $CHCl_3$ > toluene ~ THF ~ acetone. These results suggest that the two species, P_r and P_{fr}, are in equilibrium, and hydrogen bonding between bilindione and solvents caused shifts in the P_r–P_{fr} equilibrium. Only aprotic polar solvents can assist the formation of P_{fr}, implying that bilindione acts as a hydrogen bond donor in the interaction with the solvent. Figure 4 illustrates UV–vis spectra of **1**

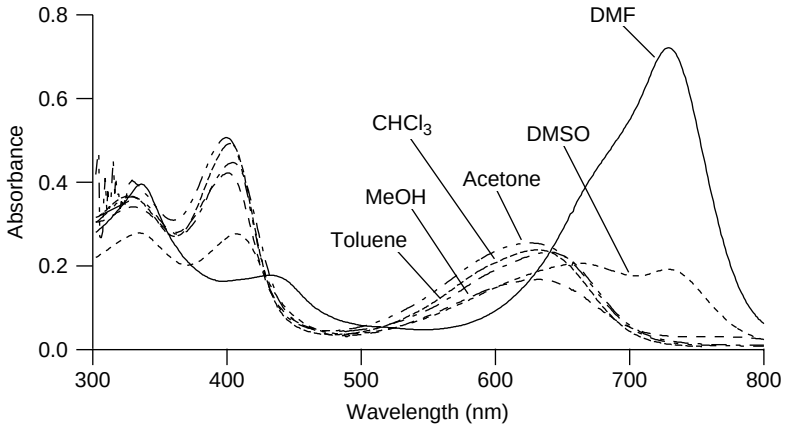

Figure 1. UV–vis spectra of **1** in various solvents.

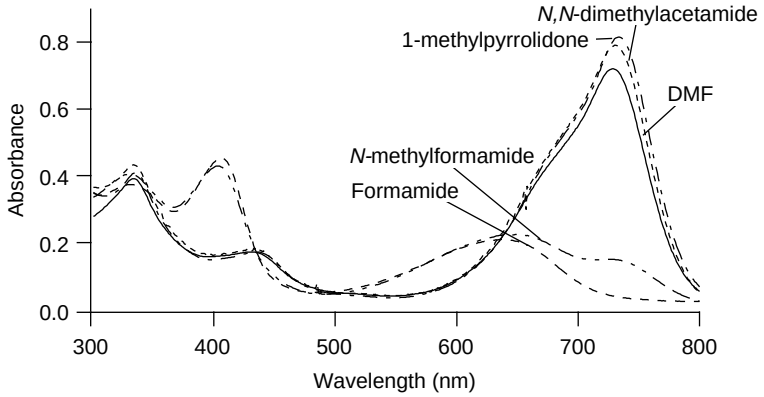

Figure 2. UV–vis spectra of **1** in various amides.

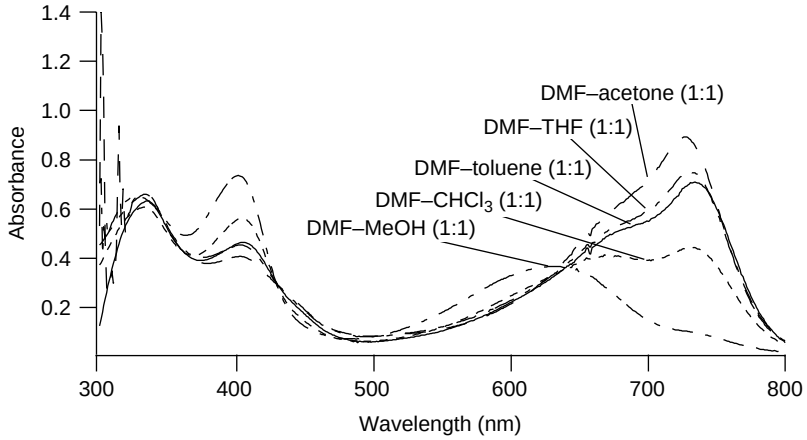

Figure 3. UV–vis spectra of **1** in mixed solvents containing DMF and co-solvents in a 1:1 (vol/vol) ratio.

in DMF-polar solvents with varying hydrogen donor properties. The P_r form is predominant when 2,2,2-trifluoroethanol (TFE), MeOH and formamide were co-solvents, while the P_{fr} form is predominant when EtOH, 2-propanol, *tert*-butanol and acetonitrile were co-solvents. The hydrogen-donating properties decrease in the order: TFE > MeOH > EtOH > 2-propanol > formamide ~ *tert*-BuOH > CH_3CN. Thus, hydrogen donor properties

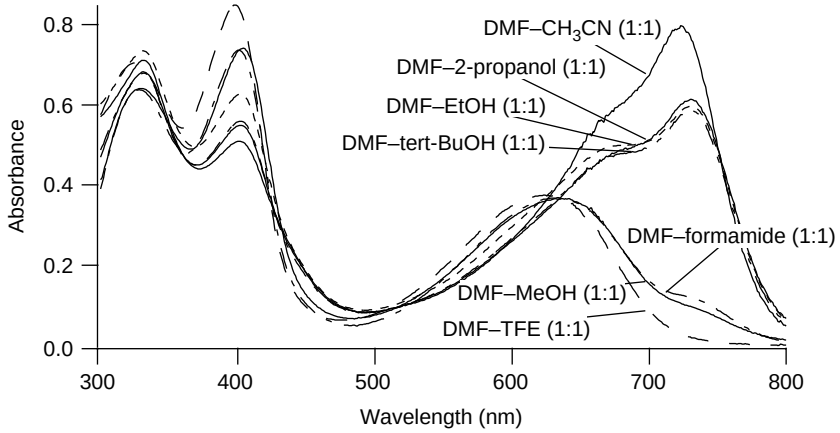

Figure 4. UV–vis spectra of **1** in mixed solvents containing DMF and polar solvents with varying hydrogen donor properties in a 1:1 (vol/vol) ratio.

Table 1. Binding constants K and UV–vis spectra of **1**–amine complexes in toluene, $CHCl_3$, THF or MeOH.

	Toluene		$CHCl_3$		THF		MeOH	
	K (M^{-1})	λ_{max} (nm)	K (M^{-1})	λ_{max} (nm)	K (M^{-1})	λ_{max} (nm)	K (M^{-1})	λ_{max} (nm)
Butylamine	a	a	a	a	1.3	736	18	731
1,2-Ethanediamine	2.2	747	0.5	736	3.3	735	13	728
1,3-Propanediamine	2.1	747	0.1	728	6.3	735	12	727
N-Ethylbutylamine	a	a	a	a	2.3	734	23	729
Pyrrolidine	3.5	750	1.1	737	1.7	735	21	728
Piperidine	1.3	780	0.4	735	2.0	736	19	729
Triethylamine	a	a	a	a	a	a	17	727
N,*N*,*N*′,*N*′-Tetramethyl-1,2-Ethanediamine	a	a	a	a	1.4	734	16	719
Pyridine	a	a	a	a	a	a	a	a

Note: 'a' indicates no spectral changes were observed even in the presence of 1.2 M of amines.

should be one of the factors to inhibit the formation of the P_{fr} form.

2.3 UV–vis spectra of 5,10,15-tri (4-cyanophenyl)bilindione in a solution containing amines

To a solution of **1** in apolar solvents or protic solvents, 0.1–1 M of amines were added. The Q-band shifted to a longer wavelength for some amines such as butylamine, 1,2-ethanediamine, 1,3-propanediamine, *N*-ethylbutylamine, pyrrolidine, piperidine, triethylamine and *N*,*N*,*N*′,*N*′-tetramethylethylenediamine. In contrast to the solvatochromism caused by amides, both protic amines (primary amines and secondary amines) and aprotic amines (tertiary amines) caused the shift to the longer wavelength. Table 1 summarises the spectral changes upon addition of amines in toluene, $CHCl_3$, THF or MeOH and the binding constants determined by Benesi–Hildebrand plots. Among the amines, 1,2-ethanediamine, 1,3-propanediamine and pyrrolidine efficiently induced the spectral changes in the concentration of ca. 0.1 M. Spectral shifts were modest for triethylamine, and almost no shift was observed for pyridine. The spectral shifts occur more favourably in protic solvents such as MeOH. In toluene, however, the red shifts were observed for limited amines at high concentrations (~ 1 M). As typical examples, spectral titration of a solution of **1** in toluene, $CHCl_3$, THF and MeOH with 1,2-ethanediamine is shown in Figures 5–8. In toluene, spectral changes were very small, while in MeOH, much larger changes were observed by the addition of 1,2-ethanediamine.

It is noteworthy that the solvent effects are different for amides and amines. Formation of P_{fr} in a mixed solvent of aprotic amides was favourable with non-polar co-solvents, while formation of P_{fr} by the addition of amines was favourable in polar protic solvents. This could be ascribed to the different nature of the P_{fr} species formed in amides and amines. One of the possible interaction modes is that the proton-transferred hydrogen bonding (*6*) occurs for the amine–bilindione system in polar protic solvents, where the ionic nature of the hydrogen-bonding complex can be stabilised in polar solvents (Scheme 2). Several studies

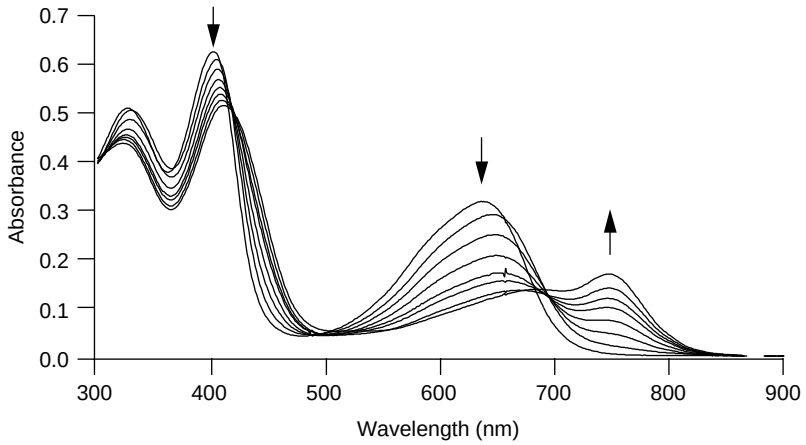

Figure 5. UV–vis spectral changes of **1** in toluene. [1,2-ethanediamine] = 0, 0.12, 0.24, 0.35, 0.46, 0.58, 0.69, 0.79 M. Arrows indicate increasing order of 1,2-ethanediamine. Binding constant determined by the Benesi–Hildebrand plot was 2.2 M^{-1}.

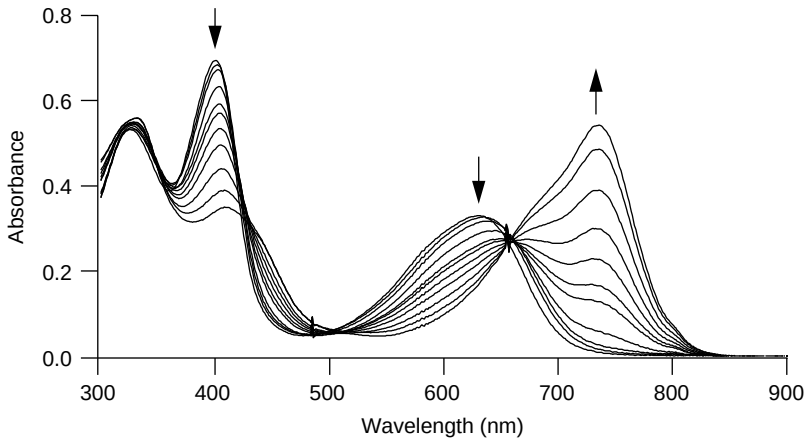

Figure 6. UV–vis spectral changes of **1** in $CHCl_3$ upon addition of 1,2-ethanediamine. [1,2-ethanediamine] = 0, 0.29, 0.58, 0.35, 0.46, 0.58, 0.69, 0.79 M. Arrows indicate increasing order of 1,2-ethanediamine. Binding constant determined by the Benesi–Hildebrand plot was 0.54 M^{-1}.

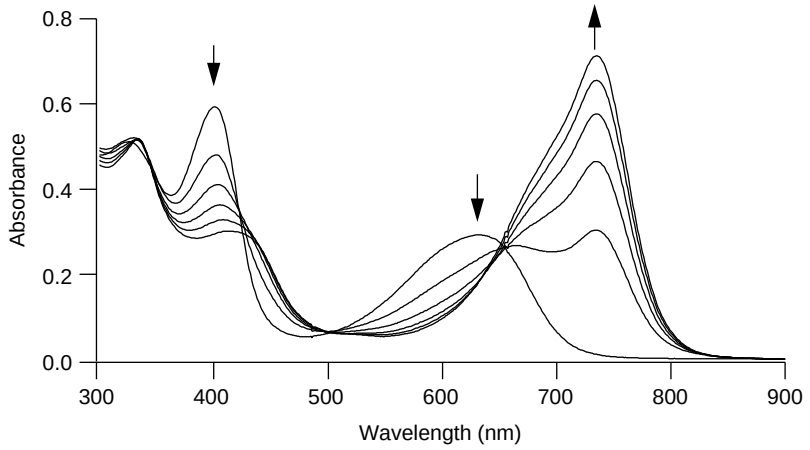

Figure 7. UV–vis spectral changes of **1** in THF upon addition of 1,2-ethanediamine. [1,2-ethanediamine] = 0, 0.12, 0.24, 0.35, 0.46, 0.58 M. Arrows indicate increasing order of 1,2-ethanediamine. Binding constant determined by the Benesi–Hildebrand plot was 3.2 M^{-1}.

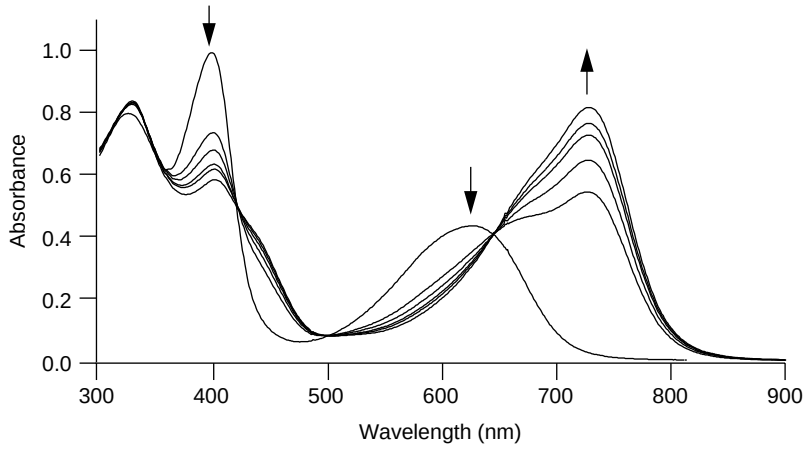

Figure 8. UV–vis spectral changes of **1** in MeOH upon addition of 1,2-ethanediamine. [1,2-ethanediamine] = 0, 0.12, 0.24, 0.35, 0.46, 0.58 M. Arrows indicate increasing order of 1,2-ethanediamine. Binding constant determined by the Benesi–Hildebrand plot was 12.5 M^{-1}.

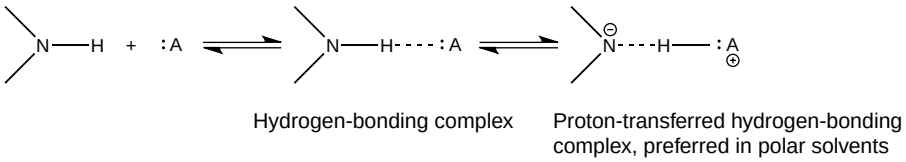

Scheme 2. Normal hydrogen-bonding complex and proton-transferred hydrogen-bonding complex. ═N—H denotes the D-ring pyrrolic imino group of bilindione, and A denotes a hydrogen bond acceptor molecule.

revealed that the hydrogen-bonding complex between *p*-nitrophenol and amines forms favourably in polar solvents (*7*).

2.4 Comparison of solvatochromism of tri(4-cyanophenyl)bilindione with that of tri(4-methoxyphenyl)bilindione

We compared the solvatochromism between the two bilindiones with either electron-donating methoxy groups (**2**) or electron-withdrawing cyano groups (**1**) in the aryl groups. UV–vis spectra of **2** and **1** in mixed solvents of DMF and $CHCl_3$ are shown in Figures 9 and 10. Absorbance at 730 nm due to the P_{fr} species was plotted against the fraction of $CHCl_3$ in Figure 11. Figure 11 shows that smaller amounts of $CHCl_3$ can inhibit the formation of P_{fr} of **2** than that of **1**. Therefore, formation of the P_{fr} species is more favourable in **1** bearing electron-withdrawing groups. This implies that bilindione would serve as a hydrogen donor when it interacted with DMF.

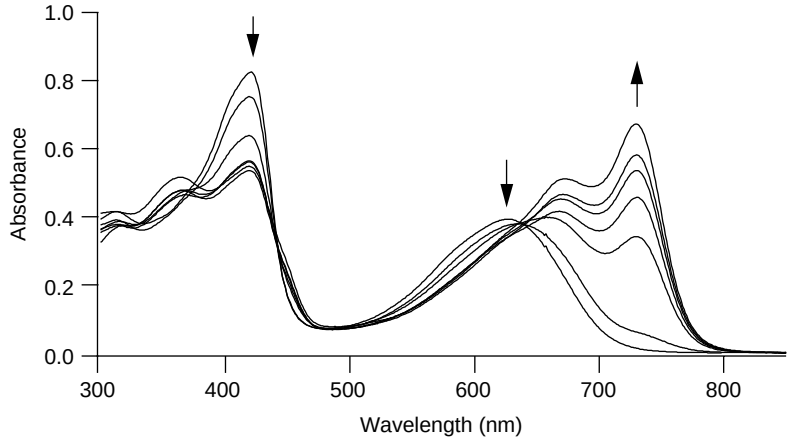

Figure 9. UV–vis spectra of **2** in mixed solvents: $CHCl_3$, $CHCl_3$–DMF (1:1), $CHCl_3$–DMF (1:3), $CHCl_3$–DMF (1:5), $CHCl_3$–DMF (1:7), $CHCl_3$–DMF (1:9) and DMF. Arrows indicate increasing order of DMF.

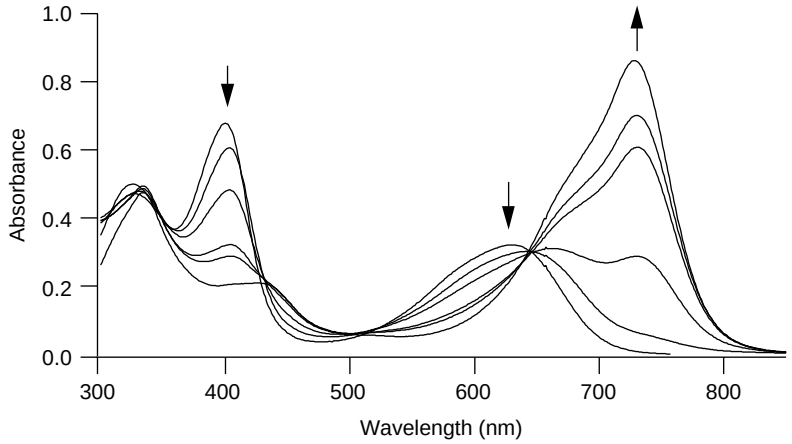

Figure 10. UV–vis spectra of **1** in mixed solvents: $CHCl_3$, $CHCl_3$–DMF (2:1), $CHCl_3$–DMF (1:1), $CHCl_3$–DMF (1:2), $CHCl_3$–DMF (1:3) and DMF. Arrows indicate increasing order of DMF.

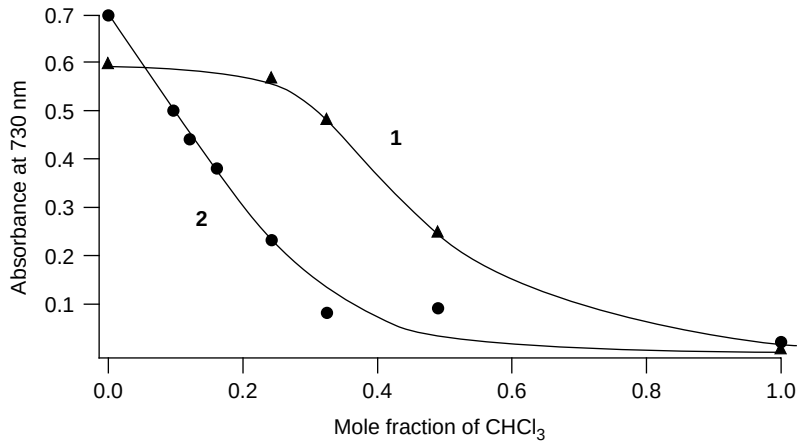

Figure 11. Plot of the absorbance at 730 nm of **1** and **2** in DMF–$CHCl_3$ mixed solvents against mole fraction of $CHCl_3$. Data are taken from Figures 9 and 10.

The interaction mode that the amide acts as a hydrogen acceptor is consistent with the observation that formation of P_{fr} was only observed for aprotic amides. We do not have any conclusive evidence which hydrogen atom of **1** is involved in hydrogen bonding. One of the candidates for the hydrogen donor NH is the D-ring NH, since other NH

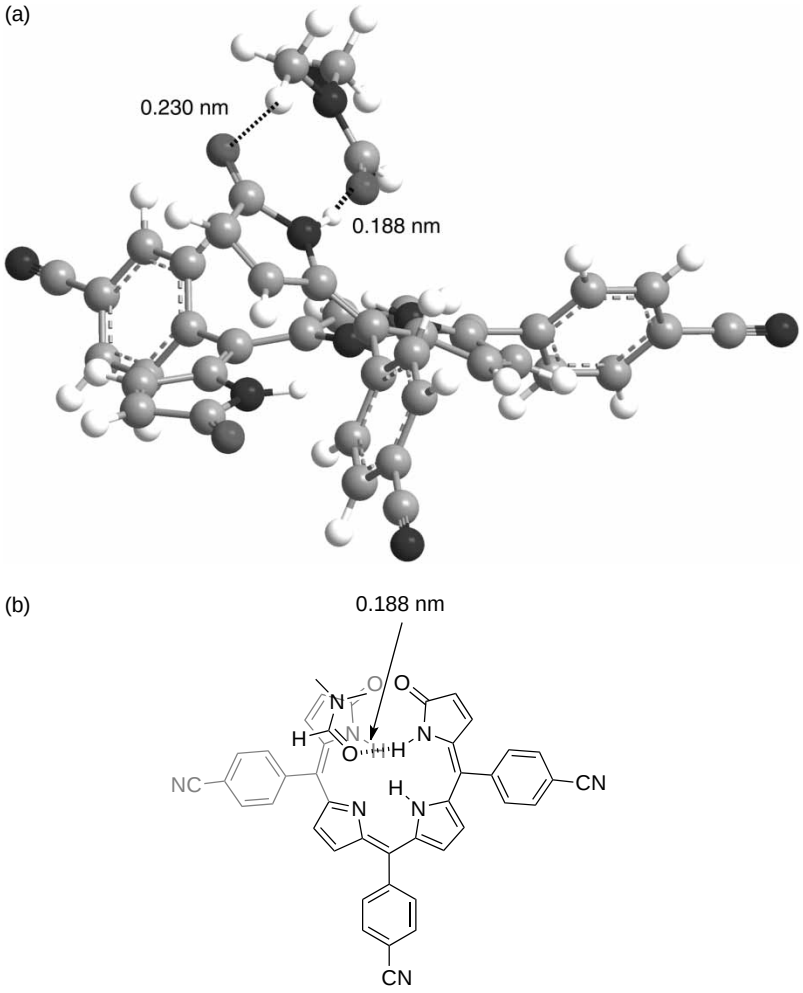

Figure 12. (a) Optimised structure of the **1**–DMF complex at the B3LYP/6-31G(d) level. (b) Schematic representation of the complex.

hydrogens are intramolecularly hydrogen-bonded to the imino N of the B-ring pyrrole.

2.5 MO calculations of the possible complex structures and excited states

To understand possible interactions causing solvatochromism, we performed molecular orbital calculations (*8*) of the optimised structures of tricyanobilindione **1**, a **1**–DMF complex, the anion and the cation of **1** at the B3LYP/6-31G(d) levels and the excited states were calculated using time-dependent DFT (*9*).

The optimised structure of the **1**–DMF complex is shown in Figure 12. The distance between the D-ring NH hydrogen and the carbonyl oxygen of DMF was 0.188 nm. The complex formation is an exothermic reaction of 14.0 kcal/mol on the basis of the energy difference between the complex, **1** and DMF at the B3LYP/6-31G(d) level. The enthalpy change can be attributed to both hydrogen bonding and van der Waals interactions.

Time-dependent DFT calculations of the excited states revealed that the absorption maxima and the oscillator strength of **1**, the **1**–DMF complex, deprotonated **1** at the D-ring NH: $(\mathbf{1} - \mathrm{H})^-$, and protonated **1** at B-ring N: $(\mathbf{1} + \mathrm{H})^+$ are 620.2 ($f = 0.24$), 640.1 ($f = 0.25$), 746.7 ($f = 0.25$) and 691.2 nm ($f = 0.31$), respectively. According to the MO calculations, hydrogen bonding caused only a modest red shift in the Q-band, and complete deprotonation caused a considerable red shift. Stanck and Grubmayr (*10*) suggested that the anion of 2,3-dihydrobilindione is a model of the P_{fr} form of phytochrome, since the absorption maximum of 2,3-dihydrobilindione shifted from 582 to 784 nm upon addition of a base. The solvatochromism observed for **1** and **2** implies that hydrogen-bonding interaction can induce similar spectral shifts in the chromophore of bilindiones, although the chromophore was not deprotonated. Thus, the present study suggests that the appropriate arrangement of the hydrogen bond donor group in the protein can alter the excited states of bilindione to result in the spectral shifts.

3. Experimental

UV–vis spectra were recorded on an Agilent 8453 UV–vis spectrometer at 298 K. $[\mathbf{1}] = 3.0 \times 10^{-5}$ M.

Bilindiones **1** and **2** were prepared from the iron porphyrins using coupled oxidation (*4*).

(4*Z*,9*Z*,15*Z*)-5,10,15-tri(4-cyanophenyl)-(21*H*, 23*H*, 24*H*)-1,19,21,24-tetrahydro-1,19-bilindione (**1**): ^{1}H NMR (500 MHz, chloroform-*d*): $\delta = 6.33$ (d, $J = 5.80$ Hz, 2H), 6.50 (d, $J = 4.35$ Hz, 2H), 6.70 (d, $J = 4.35$ Hz, 2H), 7.01 (d, $J = 5.80$ Hz, 2H), 7.51 (d, 4H, $J = 8.00$ Hz), 7.64 (d, $J = 7.95$ Hz, 2H), 7.70 (d, $J = 8.00$ Hz, 4H), 7.82 (d, $J = 7.95$ Hz). MS (MALDI-TOF): $m/z = 635$ [MH^+]; UV–vis spectrum λ_{max} (ε_{max}): 400 nm ($2.59 \times 10^4\,M^{-1}\,cm^{-1}$), 631 nm ($1.26 \times 10^4\,M^{-1}\,cm^{-1}$).

(4*Z*,9*Z*,15*Z*)-5,10,15-tri(4-methoxycarbonylphenyl)-(21*H*,23*H*,24*H*)-1,19,21,24-tetrahydro-1,19-bilindione (**2**): ^{1}H NMR (500 MHz, chloroform-*d*): $\delta = 3.85$ (s, 6H), 3.97 (s, 3H), 6.26 (d, $J = 5.8$ Hz, 2H), 6.47 (d, $J = 4.55$ Hz, 2H), 6.69 (d, $J = 4.55$ Hz, 2H), 6.94 (d, $J = 5.8$ Hz, 2H), 7.45 (d, $J = 8.45$ Hz, 4H), 7.60 (d, $J = 8.40$ Hz, 2H), 8.04 (d, $J = 8.45$ Hz, 4H), 8.17 (d, $J = 8.45$ Hz, 2H). MS (MALDI-TOF): $m/z = 732$ [M^+]; UV–vis spectrum: λ_{max} (ε_{max}): 328 nm ($2.56 \times 10^4\,M^{-1}\,cm^{-1}$), 399 nm ($3.86 \times 10^4\,M^{-1}\,cm^{-1}$), 626 nm ($2.08 \times 10^4\,M^{-1}\,cm^{-1}$).

Acknowledgements

This work was supported by 'Creating Research Center for Advanced Molecular Biochemistry', Strategic Development of Research Infrastructure for Private Universities, the Ministry of Education, Culture, Sports, Science and Technology (MEXT), Japan.

References

(1) (a) Falk, H. *The Chemistry of Linear Oligopyrroles and Bile Pigments*; Springer-Verlag: Vienna, New York, 1989. (b) Mizutani, T.; Yagi, S. *J. Porphyrins Phthalocyanines* **2004,** *8*, 226–237.

(2) (a) Ruediger, W.; Thuemmler, F. *Angew. Chem., Int. Ed.* **1991,** *30*, 1216–1228. (b) Bongards, C.; Gärtner, W. *Acc. Chem. Res.* **2010,** *43*, 485–495.

(3) Lemberg, R. *Biochem. J.* **1935**, *29*, 1322–1336.

(4) Yamauchi, T.; Mizutani, T.; Wada, K.; Horii, S.; Furukawa, H.; Masaoka, S.; Chang, H.-C.; Kitagawa, S. *Chem. Commun.* **2005**, 1309–1311.

(5) Falk, H.; Vormayr, G.; Margulies, L.; Mazur, Y.; Metz, S. *Monatsh. Chem.* **1986**, *117*, 849–858.

(6) (a) Mizutani, T.; Takagi, H.; Hara, O.; Horiguchi, T.; Ogoshi, H., *Tetrahedron Lett.* **1997,** *38*, 1991–1994. (b) Mizutani, T.; Takagi, H.; Ueno, Y.; Yamamura, K.; Ogoshi, H. *J. Phys. Org. Chem.* **1998,** *11*, 737–742. (c) Takagi, H.; Mizutani, T.; Horiguchi, T.; Kitagawa, S.; Ogoshi, H. *Org. Biomol. Chem.* **2005,** *3*, 2091–2094. (d) Etxebarria, J.; Degenbeck, H.; Felten, A.-S.; Serres, S.; Nieto, N.; Vidal-Ferran, A. *J. Org. Chem.* **2009,** *74*, 8794–8797.

(7) (a) Baba, H.; Matsuyama, A.; Kokubun, H. *J. Chem. Phys.* **1964,** *41*, 895–896. (b) Libus, W.; Mecik, M.; Sulek, W. *J. Soln Chem.* **1977,** *6*, 865–879. (c) Dwivedi, P.C.; Banga, A.K.; Sharma, N. *Spectrochim. Acta* **1986,** *42A*, 623–629. (d) Hanessian, S.; Gomtsyan, A.; Simard, M.; Roelens, S. *J. Am. Chem. Soc.* **1995,** *117*, 7630–7645. (e) Scott, R.; Vinogradov, S. *J. Phys. Chem.* **1969,** *73*, 1890–1897.

(8) Frisch, M.J.; Trucks, G.W.; Schlegel, H.B.; Scuseria, G.E.; Robb, M.A.; Cheeseman, J.R.; Scalmani, G.; Barone, V.; Mennucci, B.; Petersson, G.A.; Nakatsuji, H.; Caricato, M.; Li, X.; Hratchian, H.P.; Izmaylov, A.F.; Bloino, J.; Zheng, G.; Sonnenberg, J.L.; Hada, M.; Ehara, M.; Toyota, K.; Fukuda, R.; Hasegawa, J.; Ishida, M.; Nakajima, T.; Honda, Y.; Kitao, O.; Nakai, H.; Vreven, T.; J.A. Montgomery, J.; Peralta, J.E.; Ogliaro, F.; Bearpark, M.; Heyd, J.J.; Brothers, E.; Kudin, K.N.; Staroverov, V.N.; Kobayashi, R.;

Normand, J.; Raghavachari, K.; Rendell, A.; Burant, J.C.; Iyengar, S.S.; Tomasi, J.; Cossi, M.; Rega, N.; Millam, J.M.; Klene, M.; Knox, J.E.; Cross, J.B.; Bakken, V.; Adamo, C.; Jaramillo, J.; Gomperts, R.; Stratmann, R.E.; Yazyev, O.; Austin, A.J.; Cammi, R.; Pomelli, C.; Ochterski, J.W.; Martin, R.L.; Morokuma, K.; Zakrzewski, V.G.; Voth, G.A.; Salvador, P.; Dannenberg, J.J.; Dapprich, S.; Daniels, A.D.; Farkas, O.; Foresman, J.B.; Ortiz, J.V.; Cioslowski, J.; Fox, D.J. *Gaussian 09, Revision A.02*, Gaussian, Inc.: Wallingford, CT, 2009.

(9) Matute, R.A.; Contreras, R.; Gonzalez, L. *J. Phys. Chem. Lett.* **2010**, *1*, 796–801.

(10) Stanek, M.; Grubmayr, K. *Chem. Eur. J.* **1998**, *4*, 1660–1666.